Catalysis Today 149 (2010) 11–18

Contents lists available at ScienceDirect

Catalysis Today

journal homepage: www.elsevier.com/locate/cattod

# Effect of $TiO_2$ on hydrodenitrogenation performances of MCM-41 supported molybdenum phosphides

Xinping Duan [a], Xiang Li [a,b], Anjie Wang [a,b,*], Yang Teng [a], Yao Wang [b], Yongkang Hu [a,b]

[a] State Key Laboratory of Fine Chemicals, Department of Catalysis, Dalian University of Technology, 158 Zhongshan Road, Dalian 116012, PR China
[b] Liaoning Key Laboratory of Petrochemical Technology and Equipments, Dalian University of Technology, 158 Zhongshan Road, Dalian 116012, PR China

ARTICLE INFO

*Article history:*
Available online 28 May 2009

*Keywords:*
Molybdenum phosphide
$TiO_2$
Hydrodenitrogenation
Quinoline
Decahydroquinoline
Promoter

ABSTRACT

The effect of $TiO_2$ on the hydrodenitrogenation (HDN) performance of MoP/MCM-41 was investigated using quinoline and decahydroquinoline as the model molecules. The catalysts were characterized by XRD, CO chemisorption, TEM, TPR and pyridine FT-IR. Addition of $TiO_2$ enhanced the C–N bond cleavage activity of MoP/MCM-41 but inhibited its dehydrogenation activity. A maximum HDN activity was observed when the $TiO_2$ loading was 5 wt%. The characterization results indicated that introduction of $TiO_2$ did not affect the formation of MoP phase. The $TiO_2$-containing catalysts possessed higher CO uptake than MoP/MCM-41, but no significant differences in the acid properties and particle size distributions were observed for all the catalysts. XPS results revealed a surface enrichment of $TiO_2$ in Ti-containing catalysts and small amount of these surface $TiO_2$ can be partially reduced to $Ti^{n+}$ ($n < 4$). It is suggested that these $Ti^{n+}$ ($n < 4$) species may be responsible for the promoting effect of $TiO_2$ on the HDN performance of MoP/MCM-41.



## 1. Introduction

The conventional hydrodesulfurization (HDS) and hydrodenitrogenation (HDN) catalysts are alumina-supported Mo or W sulfides promoted by Ni or Co [1]. Generally, HDN is more difficult than HDS over these supported metal sulfides [2]. The increasingly strict environment regulations have stimulated research on high performance HDS and HDN catalysts. Among the approaches to achieve this goal, developing novel catalyst other than bimetallic sulfides is a promising one.

Recently, transition-metal phosphides have attracted great attention as a new class of high-performance HDS and HDN catalysts [3–8]. Zuzaniuk and Prins [8] as well as Stinner et al. [9] investigated the HDN of *o*-propylaniline over unsupported and supported MoP, $Ni_2P$, $Co_2P$, WP, NiMoP, and CoMoP catalysts in the absence and presence of $H_2S$. They found that the cobalt compounds, $Co_2P$ and CoMoP, were the least active catalysts, whereas MoP showed the highest HDN activity. Moreover, MoP catalysts also exhibited higher sulfur resistance than other phosphides.

MoP is a metallic conductor with properties similar to ordinary intermetallic compounds with a hexagonal WC-type structure [10]. Besides the high HDN activity, MoP also showed a substantial improvement for HDS as compared to the molybdenum sulfide catalysts [10–13]. However, unlike molybdenum sulfide, introduction of a secondary metal in MoP, such as Co or Ni, leads to reduction of HDS and HDN activity. Zuzaniuk and Prins [8] and Rodriguez et al. [11] reported that CoMoP and NiMoP had lower HDN activities than $Ni_2P$ and MoP catalysts. Similarly, Sun et al. [14] studied the HDS of dibenzothiophene (DBT) over silica-supported MoP, $Ni_2P$ and NiMoP catalysts, but no synergetic effect was observed between the phosphided Ni and Mo atoms. Only recently, Abu and Smith [15] reported that introduction of a small amount of Co to bulk $Ni_2P$ and MoP led to a significant increase in the direct desulfurization pathway selectivity in the conversion of 4,6-dimethyldibenzothiophene. They proposed that the change in selectivity corresponded to the change in the surface Brönsted acidity and the metal sites. They also investigated the HDN of carbazole over $Ni_x$MoP [16], but found that $Ni_x$MoP had a lower turnover frequency (TOF).

Generally, the HDS activity of CoMo or NiMo sulfides supported on $TiO_2$-$Al_2O_3$ mixed oxides is superior to that of conventional $\gamma$-$Al_2O_3$ supported CoMo or NiMo sulfides [17]. Under these circumstances, $TiO_2$ also acts as a promoter. The addition of $TiO_2$ to $\gamma$-$Al_2O_3$ could improve the reducibility and sulfidability of Mo-based catalysts. Ramírez et al. [18] suggested that $TiO_2$ was an electronic promoter in HDS catalysts. The 3d electron in $Ti^{3+}$ formed under the HDS reaction conditions can be transferred through the conduction band of the support and injected into the Mo 3d

* Corresponding author at: School of Chemical Engineering, Dalian University of Technology, Dalian 116012, PR China. Tel.: +86 411 39893693; fax: +86 411 39893693.
*E-mail address:* ajwang@dlut.edu.cn (A. Wang).

0920-5861/$ – see front matter © 2009 Elsevier B.V. All rights reserved.
doi:10.1016/j.cattod.2009.04.014

conduction band, thus leading to weakening of the Mo–S bond and an increase in the number of S vacancies. Our recent results [19] indicated that $TiO_2$ is a promising promoter for $Ni_2P$ in quinoline (Q) and decahydroquinoline (DHQ) HDN, enhancing both the hydrogenation and C–N bond cleavage activities of $Ni_2P$. In the present study, the effect of $TiO_2$ on the HDN performance of MoP/MCM-41 was studied using Q and DHQ as the model molecules.

## 2. Experimental

### 2.1. Catalyst preparation

Siliceous MCM-41 was synthesized using sodium silicate as the silica source and cetyltrimethylammonium bromide as the template, following the procedure in a previous paper [20]. The synthesized siliceous MCM-41 has a specific surface area of 1028 $m^2\,g^{-1}$, a pore volume of 0.90 $cm^3\,g^{-1}$, and a BJH average pore size of 3.4 nm.

The MoP/MCM-41 precursor was prepared by impregnating MCM-41 with an aqueous solution of $(NH_4)_2HPO_4$ and $(NH_4)_6Mo_7O_{24}{\cdot}4H_2O$. The precursors of MoP-Ti($x$)/MCM-41 and Ti($x$)-MoP/MCM-41, in which $x$ represents the weight concentration of $TiO_2$ in the precursors, were prepared by a successive impregnation procedure. MoP-Ti($x$)/MCM-41 refers to the catalyst prepared by impregnation of Ti species followed by the impregnation of Mo and P components, while Ti($x$)-MoP/MCM-41 represents the catalyst prepared by the impregnation of Mo and P species followed by the impregnation of Ti species. The preparation procedure of Ti($x$)-MoP/MCM-41 catalyst is described as follows. 3.56 g $(NH_4)_2HPO_4$ (A.R. grade) and 2.57 g $(NH_4)_6Mo_7O_{24}{\cdot}4H_2O$ (A.R. grade) (Mo/P = 1) was dissolved in 10 mL deionized water to form a clear solution. 4 g siliceous MCM-41 was wet-impregnated with the above solution for 8 h. After evaporation of water, the solid material was dried at 120 °C for 10 h, and then calcined in air at 500 °C for 3 h to obtain the oxidic precursor of MoP/MCM-41. The MoP/MCM-41 precursor was then impregnated by a solution of tetrabutyl titanate in ethanol for 12 h. The resulting solid was dried at 120 °C for 8 h and calcined in air at 500 °C for 6 h to obtain the precursor of Ti($x$)-MoP/MCM-41. MoP-Ti($x$)/MCM-41 catalyst was prepared according the following procedure: MCM-41 sample was impregnated in an ethanol solution of tetrabutyl titanate for 12 h. The resulting solid was dried at 120 °C for 8 h and calcined in air at 500 °C for 6 h to obtain the support Ti($x$)/MCM-41. Ti($x$)/MCM-41 was impregnated with an aqueous solution of $(NH_4)_2HPO_4$ and $(NH_4)_6Mo_7O_{24}{\cdot}4H_2O$, followed by drying at 120 °C for 10 h and calcination in air at 500 °C for 3 h. For all the samples, the total loading of $MoO_3$ and $P_2O_5$ in the oxidic precursor was 40 wt%, and the Mo/P atomic ratio was 1.0.

### 2.2. Catalyst characterization

TPR profiles of the MoP/MCM-41, Ti(5)-MoP/MCM-41 and MoP-Ti(5)/MCM-41 precursors were measured on a Chembet-3000 analyzer. Before the measurement, the sample (0.10 g) was pretreated in He at 200 °C for 2 h. A gas mixture of 10% $H_2$ in Ar was used as the reacting agent, and the TPR profiles of the catalysts were measured from 100 to 1000 °C at 5 °C $min^{-1}$.

The XRD patterns of MoP/MCM-41, Ti(5)-MoP/MCM-41 and MoP-Ti(5)/MCM-41 were measured on a Rigaku D/Max 2400 diffractometer using nickel-filtered Cu Kα radiation at 40 kV and 100 mA. The IR spectra of pyridine adsorbed on the catalysts were recorded using an Equinox55 instrument. Before pyridine adsorption, the sample was subjected to vacuum in the sample holder at 450 °C for 4 h until a pressure of $7 \times 10^{-4}$ Pa was reached. After heat treatment at 150 °C in vacuum, the IR spectrum was measured *in situ*. The transmission electron microscope (TEM) images of MoP/MCM-41, Ti(5)-MoP/MCM-41 and MoP-Ti(5)/MCM-41 were acquired on a JEOL 2010 microscope operating at 200 kV. Before the XRD, TEM and IR measurements, all the samples were prepared by a temperature-programmed reduction method, followed by passivation with 0.5% $O_2$ in Ar.

X-ray photoelectron spectroscopy (XPS) spectra of the MoP/MCM-41, MoP-Ti(5)/MCM-41 and Ti(5)-MoP/MCM-41 catalysts were acquired with a Multilab2000 X-ray photoelectron spectrometer, using a Mg Kα source. All binding energies were referenced to the C 1s peak at 284.6 eV.

CO chemisorption was measured using a Chembet-3000 analyzer according to the literature [15]. An amount of 0.2 g passivated sample was reduced in a $H_2$ flow to remove the passivation layer (80 mL $min^{-1}$ flow rate, heating from 25 to 650 °C at 10 °C $min^{-1}$ and then holding for 1 h). Pulses of 1% CO in Ar were injected until a steady breakthrough was achieved. The CO uptake of the sample was calculated according to the accumulated difference in the peak areas of input pulses and output signals.

### 2.3. HDN activity measurement

The HDN of quinoline or DHQ was carried out using a fixed-bed reactor. Prior to HDN reaction, the oxidic precursors of the phosphides were transformed into the active phases. Instead of the conventional *ex situ* $H_2$ temperature-programmed reduction (TPR) method [4,9], an *in situ* $H_2$ TPR method was used to transform the precursor into the active phase [21]. The precursor was pelleted, crushed, and sieved to 20–30 meshes. A total of 0.20 g precursor was used for each run. The precursor was reduced in a 150 mL $min^{-1}$ $H_2$ flow by heating from room temperature to 500 °C at 5 °C $min^{-1}$, from 500 °C to 650 °C at 1 °C $min^{-1}$, and holding at 650 °C for 3 h. Then the reactor was cooled to the HDN reaction temperature. The HDN activities of the catalysts were investigated using a solution of 1 wt% quinoline or 0.8 wt% DHQ in decalin (A.R. grade) as the model fuel. The HDN reaction conditions were temperature 300–360 °C, total pressure 4 MPa, WHSV 24 $h^{-1}$, and $H_2$ flow rate 50 mL $min^{-1}$ (at atmospheric pressure). Sampling of liquid HDN products was started 6 h after the steady reaction condition was achieved. Liquid samples were collected at an interval of 20 min. The compositions of both feed and the HDN liquid products were analyzed by an Agilent-6890N gas chromatograph equipped with an FID detector using commercial HP-5 column.

Scheme 1 shows the reaction network of quinoline HDN [22]. The conversion of quinoline to 1,2,3,4-tetrahydroquinoline (THQ1) is very fast, and most likely equilibrium is reached in every experiment [23]. Because there are several nitrogen-containing intermediates in the HDN of quinoline, such as THQ1, 5,6,7,8-tetrahydroquinoline (THQ5), ortho-propylaniline (OPA), and DHQ, conversions of Q or DHQ cannot be used to represent the HDN

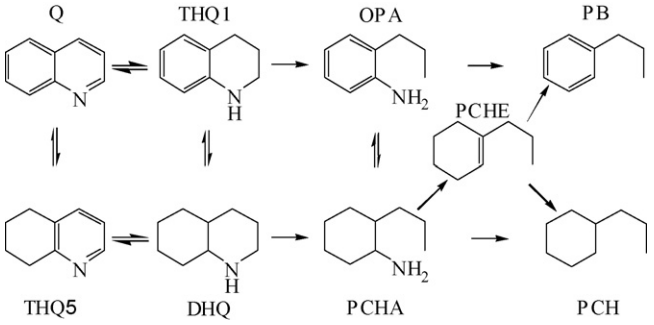


**Scheme 1.** Reaction network of quinoline HDN.

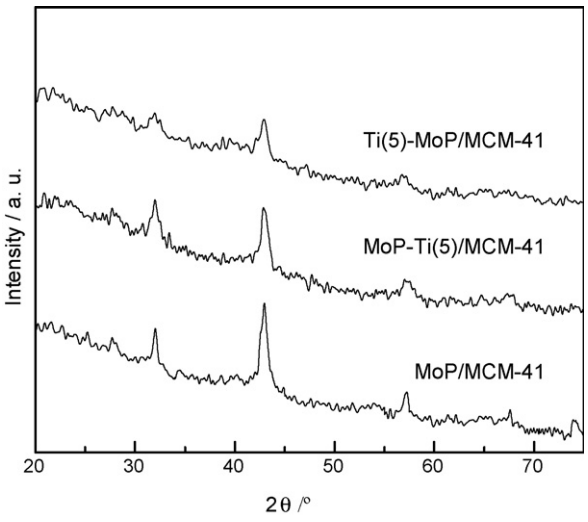


**Fig. 1.** XRD patterns of MoP/MCM-41, MoP-Ti(5)/MCM-41, and Ti(5)-MoP/MCM-41.

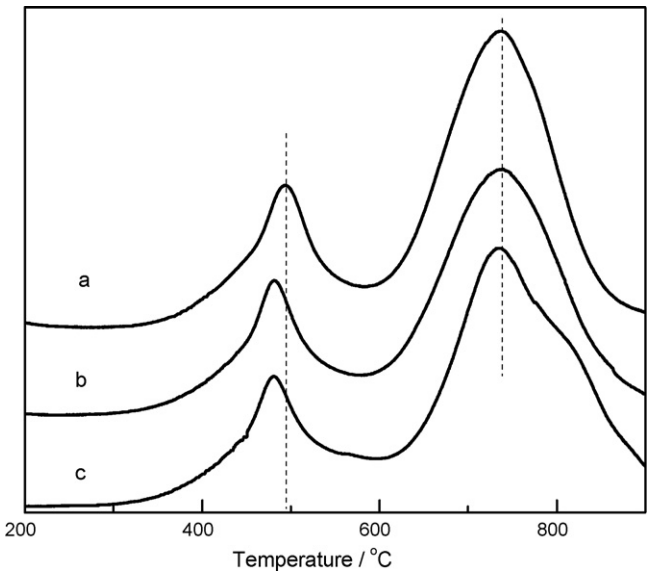


**Fig. 2.** TPR profiles of oxidic precursors of MoP/MCM-41 (a), MoP-Ti(5)/MCM-41 (b), and Ti(5)-MoP/MCM-41 (c).

efficiency. Therefore, HDN conversion was used to measure the HDN efficiency of the catalysts:

$$\text{HDN conversion} = \frac{C_{N0} - C_{NR} - C_{NC}}{C_{N0}} \times 100 = \frac{\sum C_{HC}}{C_{N0}} \times 100 \qquad (1)$$

where $C_{N0}$ represents the concentration of reactant (Q or DHQ) in the feed, $C_{NR}$ is the concentration of reactant (Q or DHQ) in the HDN liquid product, $C_{NC}$ is the sum of the concentrations of all nitrogen-containing intermediates in the HDN liquid product, and $\sum C_{HC}$ is the sum of the hydrocarbon concentrations. The HDN conversion and CO uptake were used to calculate the HDN turnover frequency (HDN TOF) of the catalysts.

## 3. Results and discussion

### 3.1. Characterization

The XRD patterns of the passivated MoP/MCM-41, MoP-Ti(5)/MCM-41 and Ti(5)-MoP/MCM-41 catalysts are shown in Fig. 1. All the samples showed only the characteristic diffraction patterns of MoP (powder diffraction file PDF24-0771). Neither lattice distortion nor peaks associated with molybdenum titanium phosphide ($Mo_{0.56}Ti_{0.44}$)P were observed. It is therefore suggested that $TiO_2$ and MoP might exist separately in MoP-Ti(5)/MCM-41 and Ti(5)-MoP/MCM-41, but not in the form of a solid solution.

The TPR profiles of the oxidic precursors of MoP/MCM-41, MoP-Ti(5)/MCM-41 and Ti(5)-MoP/MCM-41 are illustrated in Fig. 2. The temperatures of the TPR peaks are summarized in Table 1. All the samples showed two main peaks, one at low temperature (490 °C) and the other at higher temperature (730 °C). The low-temperature peak at around 490 °C corresponds to the reduction of $Mo^{6+}$ to $Mo^{4+}$, whereas the broad high-temperature peak is related to the reduction of $Mo^{4+}$ to $Mo^0$ and/or of $P^{5+}$ to $P^0$ [8]. In the presence of $TiO_2$, the low-temperature reduction peaks of MoP-Ti(5)/MCM-41 and Ti(5)-MoP/MCM-41 shifted to lower temperature, while the high-temperature reduction peaks remained almost unaffected.

The surface acidity of the supported samples was determined by FT-IR spectroscopy of pyridine adsorption. The IR spectra of pyridine adsorbed on MoP/MCM-41, MoP-Ti(5)/MCM-41 and Ti(5)-MoP/MCM-41 measured at 150 °C in the region 1700–1400 $cm^{-1}$ are shown in Fig. 3. The spectra of all the samples showed the following bands: pyridine adsorbed on Brönsted acid sites (1640 and 1540 $cm^{-1}$), Lewis acid sites (1450 and 1610 $cm^{-1}$), and the band at 1488 $cm^{-1}$, which is associated with both Brönsted and Lewis sites [24,25]. MoP/MCM-41, MoP-Ti(5)/MCM-41 and Ti(5)-MoP/MCM-41 exhibited similar surface acid properties, except that intensity of the bands at 1610 $cm^{-1}$ in the spectrum of Ti(5)-MoP/MCM-41 was lower than those of MoP/MCM-41 and MoP-Ti(5)/MCM-41, suggesting that introduction of $TiO_2$ to the surface of MoP/MCM-41 precursor led to a decrease in the number of Lewis sites.

**Table 1**
$H_2$ consumption peak temperatures of MoP/MCM-41, MoP-Ti(5)/MCM-41, and Ti(5)-MoP/MCM-41.

| Catalyst precursor | $H_2$ consumption peak temperature (°C) |
|---|---|
| MoP/MCM-41 | 493, 737 |
| MoP-Ti(5)/MCM-41 | 481, 733 |
| Ti(5)-MoP/MCM-41 | 481, 735 |

The XPS spectra in the regions of Mo 3d, P 2p, and Ti 2p for MoP/MCM-41, MoP-Ti(5)/MCM-41 and Ti(5)-MoP/MCM-41 are

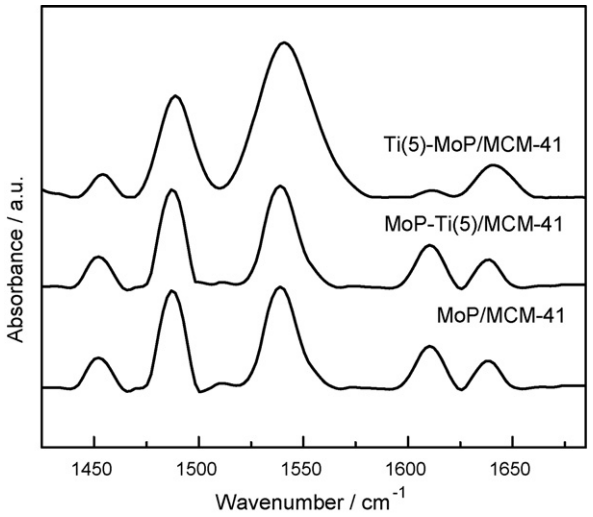


**Fig. 3.** FT-IR spectra of pyridine absorbed on MoP/MCM-41, MoP-Ti(5)/MCM-41, and Ti(5)-MoP/MCM-41.

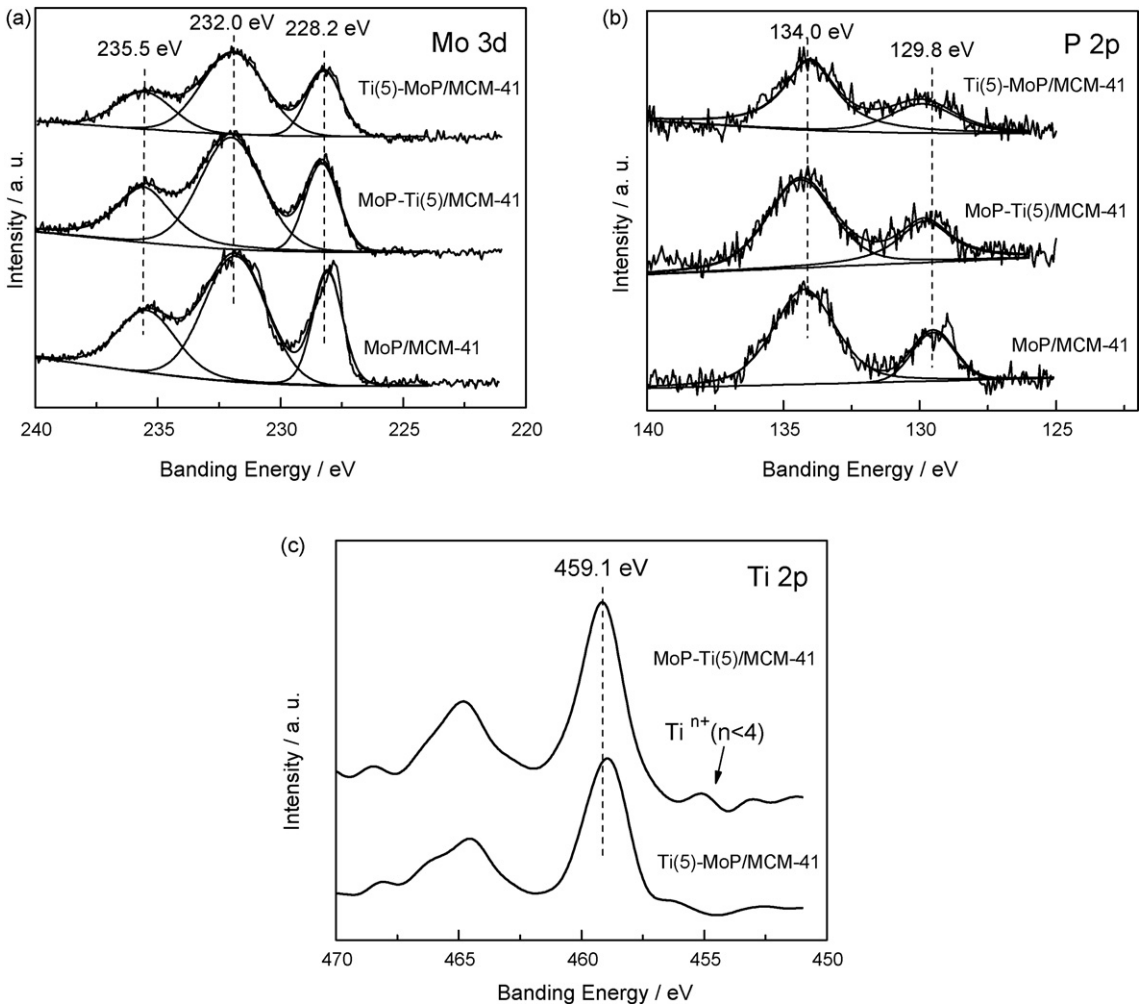


**Fig. 4.** XPS spectra of MoP/MCM-41, MoP-Ti(5)/MCM-41, and Ti(5)-MoP/MCM-41 in Mo 3d, P 2p, and Ti 2p regions.

shown in Fig. 4. All the spectra were calibrated according to the C 1 s binding energy (284.6 eV). The binding energies of Mo $3d_{5/2}$ peaks for all samples were found to be $323.0 \pm 0.3$ eV which can be ascribed to $Mo^{6+}$ [13] (Fig. 4a). The Mo $3d_{5/2}$ peaks at $228.2 \pm 0.3$ eV for MoP/MCM-41, MoP-Ti(5)/MCM-41 and Ti(5)-MoP/MCM-41 are assigned to metallic Mo species [13,15], which have a slightly higher binding energy than $Mo^0$ (227.4–227.8 eV) but lower than $Mo^{4+}$ species in $MoS_2$ (231.8 eV) [13]. The XPS spectra in the P 2p region show a large peak around 134.0 eV and a small broad peak at 129.8 eV for all three samples. The peak at 129.8 eV is associated with P bonded to Mo in MoP, while the phosphorus with a binding energy of 134.0 eV was due to the oxidized phosphorus species, such as $PO_4^{3-}$ [13,15]. In Fig. 4c, the Ti $2p_{3/2}$ peak located at 459.0–459.1 eV corresponds to the $Ti^{4+}$ species. The broad shoulder peaks presented in MoP-Ti(5)/MCM-41 and Ti(5)-MoP/MCM-41 around 455.3 eV suggested the formation of partially reduced $Ti^{n+}$ ($n < 4$) species [26]. However, it should be noted that the intensity of this peak present in the spectrum of MoP-Ti(5)/MCM-41 was higher than that observed in Ti(5)-MoP/MCM-41.

The relative surface Ti/Mo atomic ratios ($r_{XPS}$) of MoP/MCM-41 and the Ti-containing MoP/MCM-41 samples determined by XPS are summarized in Table 2. The surface Ti/Mo atomic ratios of MoP-Ti(5)/MCM-41 and Ti(5)-MoP/MCM-41 samples were much higher than the corresponding nominal values ($r_n$), indicating a surface Ti enrichment occurred for MoP-Ti(5)/MCM-41 and Ti(5)-MoP/MCM-41. Moreover, as shown in Table 2, the $r_{XPS}/r_n$ of Ti(5)-MoP/MCM-41 sample is higher than that of MoP-Ti(5)/MCM-41.

Phosphide active sites can be titrated by CO chemisorption at room temperature [27]. Irreversible CO uptake measurements were used to estimate the active sites on the catalysts. Table 2 presents the CO uptakes for MoP/MCM-41, MoP-Ti(5)/MCM-41, and Ti(5)-MoP/MCM-41. An increase in the CO uptake was observed for $TiO_2$-containing catalyst, suggesting an increase in the number of active sites with addition of $TiO_2$ to MoP/MCM-41.

TEM images of MoP/MCM-41, MoP-Ti(5)/MCM-41 and Ti(5)-MoP/MCM-41 are shown in Fig. 5. The particle sizes of all the three passivated catalysts were in the range of 4 and 7 nm.

**Table 2**
CO uptake and Ti/Mo atomic ratio of MoP/MCM-41, MoP-Ti(5)/MCM-41, and Ti(5)-MoP/MCM-41.

| Catalyst | Ti/Mo molar ratio | | $r_{XPS}/r_n$ | CO uptake ($\mu$mol $g^{-1}$) |
|---|---|---|---|---|
| | $r_n$[a] | $r_{XPS}$[b] | | |
| MoP/MCM-41 | 0 | 0 | – | 8.1 |
| MoP-Ti(5)/MCM-41 | 0.17 | 0.62 | 3.65 | 10.0 |
| Ti(5)-MoP/MCM-41 | 0.17 | 0.74 | 4.35 | 11.1 |

[a] $r_n$: The nominal Ti/Mo atomic ratio.
[b] $r_{XPS}$: The Ti/Mo atomic ratio determined by XPS.

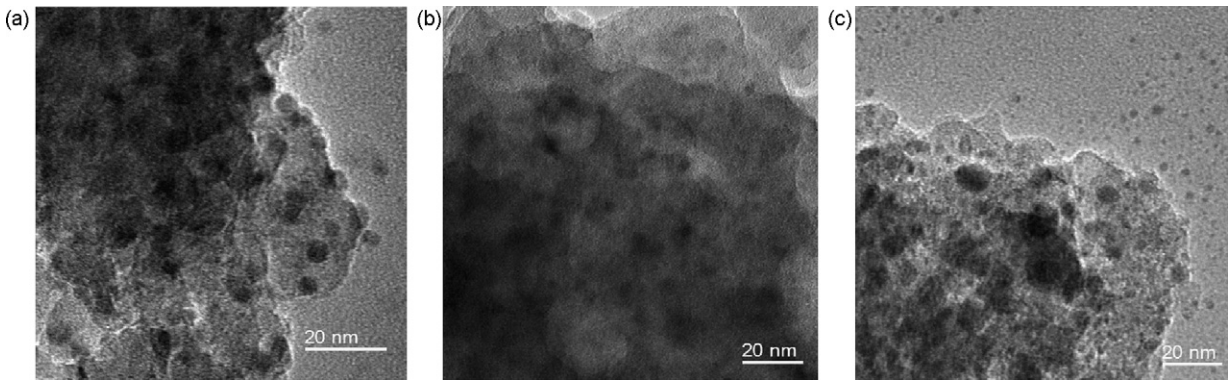


**Fig. 5.** TEM images of MoP/MCM-41 (a), MoP-Ti(5)/MCM-41 (b), and Ti(5)-MoP/MCM-41 (c).

### 3.2. HDN of quinoline

Fig. 6 shows Q HDN conversion as a function of temperature on MoP-Ti($x$)/MCM-41, Ti($x$)-MoP/MCM-41, and MoP/MCM-41. The Q HDN conversion for each catalyst increased with temperature. All the $TiO_2$-containing catalysts showed higher HDN activity than MoP/MCM-41 in the temperature range investigated. A maximum HDN activity was observed for MoP-Ti($x$)/MCM-41 or Ti($x$)-MoP/MCM-41 at a $TiO_2$ loading of 5 wt%. In the following study, we used MoP-Ti(5)/MCM-41 and Ti(5)-MoP/MCM-41 in the comparison of the HDN performance with MoP/MCM-41.

The HDN TOF of MoP/MCM-41, MoP-Ti(5)/MCM-41 and Ti(5)-MoP/MCM-41 as a function of temperature in the HDN of Q are shown in Fig. 7. The HDN TOF for all three catalysts increased with increasing temperature. The HDN TOF increased in the order: MoP/MCM-41 < Ti(5)-MoP/MCM-41 < MoP-Ti(5)/MCM-41. The HDN activity of MoP/MCM-41 was enhanced by the introduction of $TiO_2$, and it is more effective to disperse $TiO_2$ on MCM-41 than on the precursor of MoP/MCM-41.

Fig. 8 shows the variations of the reactant and liquid product distributions with reaction temperature in the Q HDN over MoP/MCM-41, MoP-Ti(5)/MCM-41 and Ti(5)-MoP/MCM-41. DHQ and PCH were the major N-containing intermediate and hydrocarbon product in Q HDN over MoP/MCM-41, respectively. The concentration of PCH increased with temperature and became the main product above 340 °C. The liquid product distributions over MoP-Ti(5)/MCM-41 and Ti(5)-MoP/MCM-41 were similar to that over MoP/MCM-41, except that more PCH but less THQ1 and DHQ were detected.

### 3.3. HDN of DHQ

Fig. 9 shows HDN TOF of MoP/MCM-41, MoP-Ti(5)/MCM-41 and Ti(5)-MoP/MCM-41 as a function of temperature in the HDN of DHQ. The HDN activities of MoP-Ti(5)/MCM-41 and Ti(5)-MoP/MCM-41 were about the same but much higher than that

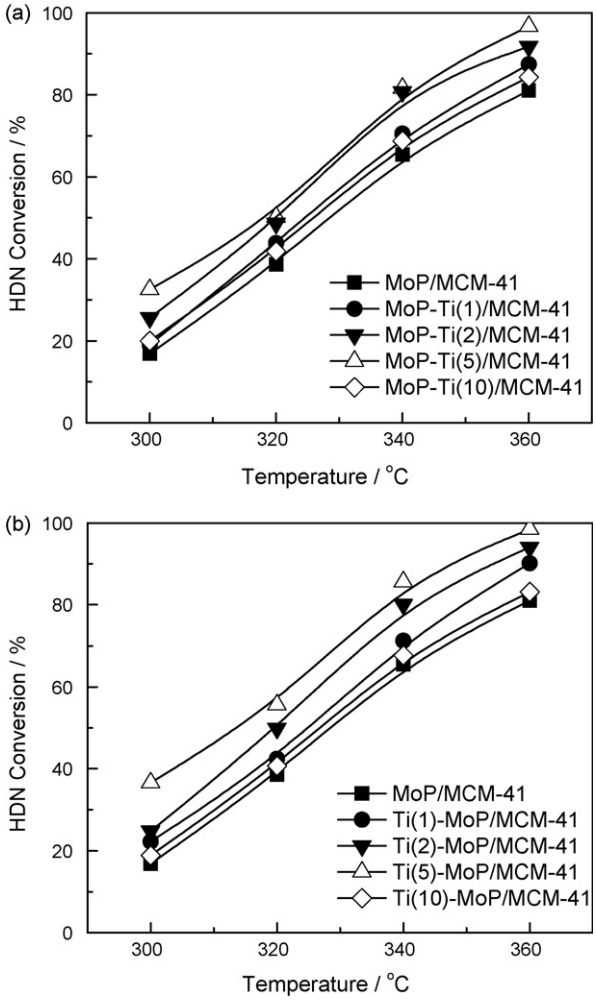


**Fig. 6.** HDN conversion as a function of temperature over MoP-Ti($x$)/MCM-41 (a) and Ti($x$)-MoP/MCM-41 (b).

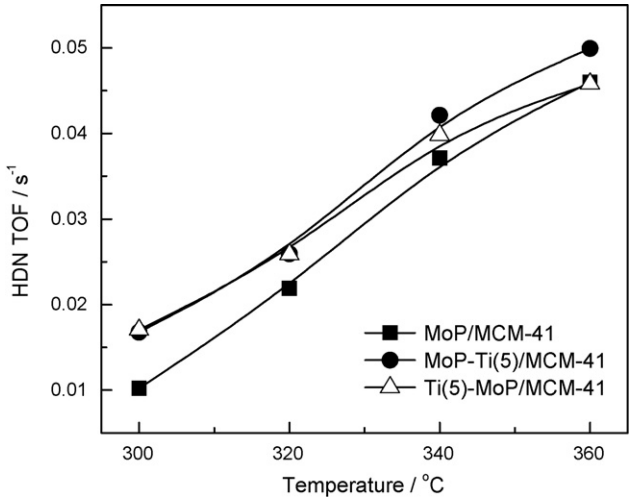


**Fig. 7.** Q HDN TOF as a function of temperature over MoP/MCM-41, MoP-Ti(5)/MCM-41, and Ti(5)-MoP/MCM-41.

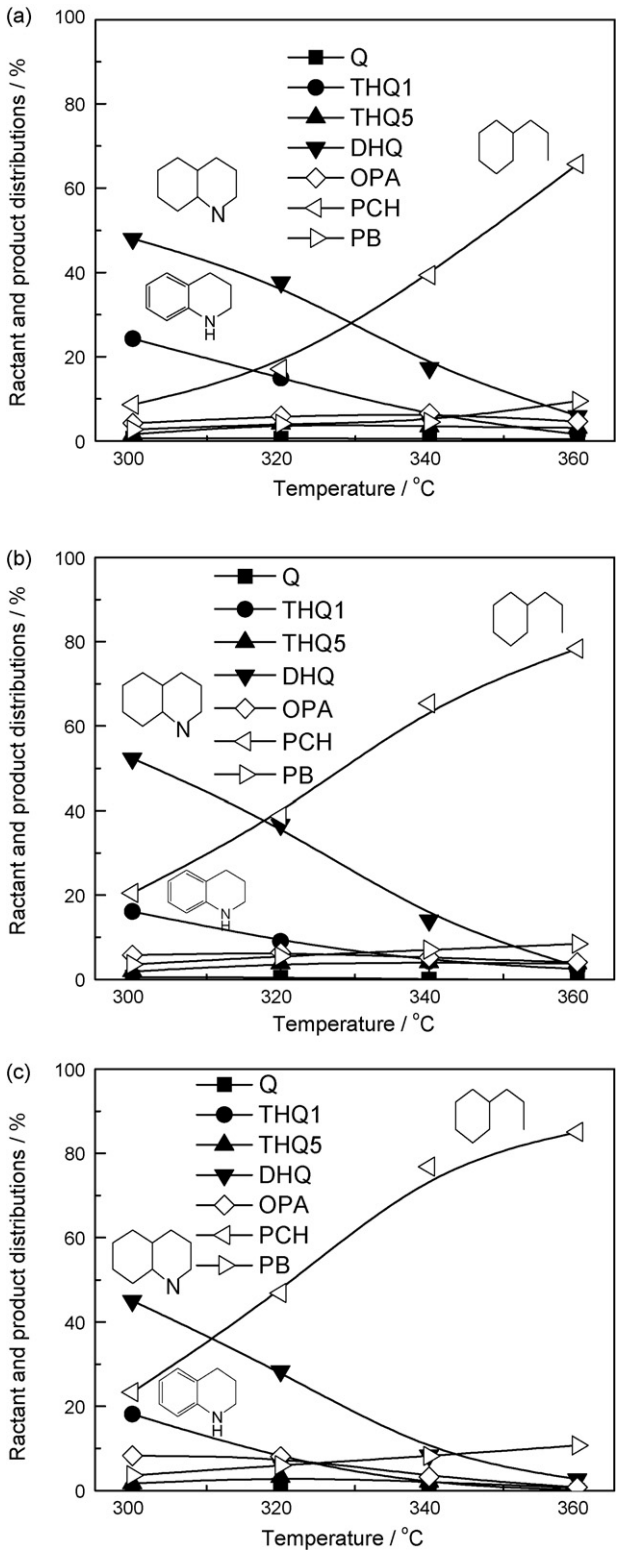


**Fig. 8.** Product distribution as a function of temperature in Q HDN over MoP/MCM-41 (a), MoP-Ti(5)/MCM-41 (b), and Ti(5)-MoP/MCM-41 (c).

of MoP/MCM-41. Fig. 10 shows that the main product of DHQ HDN over MoP/MCM-41 was PCH. THQ5, the dehydrogenation product, was observed as the second most abundant compound. MoP-Ti(5)/MCM-41 and Ti(5)-MoP/MCM-41 exhibited much higher C–N bond cleavage activity than MoP/MCM-41, because the concentration of PCH, the C–N bond cleavage product, was much higher over MoP-Ti(5)/MCM-41 and Ti(5)-MoP/MCM-41.

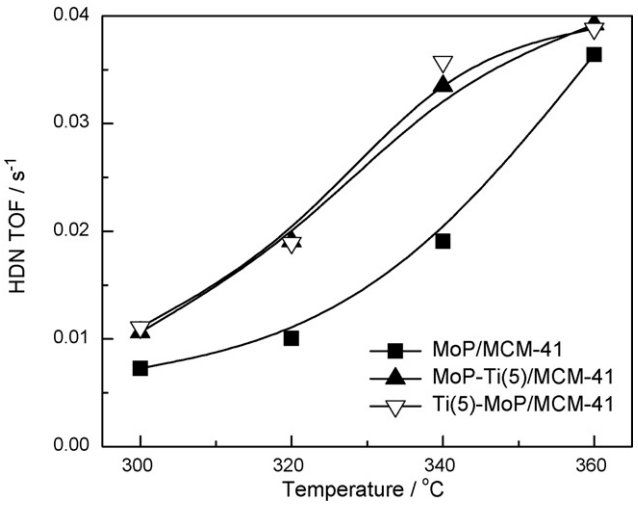


**Fig. 9.** DHQ HDN TOF as a function of temperature over MoP/MCM-41, MoP-Ti(5)/MCM-41, and Ti(5)-MoP/MCM-41.

Moreover, the formation of THQ5 was significantly reduced by the addition of $TiO_2$. Only small amount of THQ1 was detected over the Ti-containing catalysts, indicating that the dehydrogenation activity of MoP/MCM-41 was inhibited by the introduction of $TiO_2$.

## 4. Discussion

Among the methods used for preparing transition-metal phosphide hydrotreating catalysts, the temperature-programmed reduction of metal phosphates by $H_2$ is the most commonly used one. This simple method, which was described in the 19th century for the preparation of unsupported metal phosphides, was first used [3] in the preparation of metal phosphide hydrotreating catalysts. Generally, two steps are involved in the formation of transition-metal phosphides in this procedure. The first step is the reduction of the transition metal oxide at lower temperature region, and the second step is the reduction of $PO_x$ and the formation of phosphide at higher temperature. According to Rodriguez et al. [11], the reduction of $PO_x$ is the final and determining step in the formation of metal phosphides. This reaction is thermodynamically unfavorable and kinetically slow because the P–O bond is strong, and its reduction requires very low heating rate and high temperature. TPR characterization results indicated that the introduction of $TiO_2$ enhances the reduction of $Mo^{6+}$ to $Mo^{4+}$ but hardly affects the formation of MoP phase. In other words, addition of $TiO_2$ mainly affects the first step in the formation of MoP phase. This is in agreement with the results reported by Wei et al. [28]. They observed from TPR profiles that the hydrogen consumption increases with $TiO_2$ content in $TiO_2$-$Al_2O_3$ supported molybdenum-based catalysts. They suggested that $TiO_2$ promotes the reduction of molybdenum oxides to lower valence states.

The site densities of MoP/MCM-41, MoP-Ti(5)/MCM-41 and Ti(5)-MoP/MCM-41 measured by CO chemisorption (Table 2) indicated that the number of surface active sites was slightly increased by the addition of $TiO_2$. Nevertheless, this increase in the active sites cannot be attributed to the decrease in the particle size, because no marked difference in particle size was observed for these three catalysts in TEM (Fig. 5).

The Py-IR results revealed that MoP/MCM-41 possessed both Lewis and Brönsted acid sites. Addition of $TiO_2$, either to the precursor of MoP/MCM-41 or to MCM-41, had little influence on the acid properties of MoP/MCM-41. The slightly decreased number of

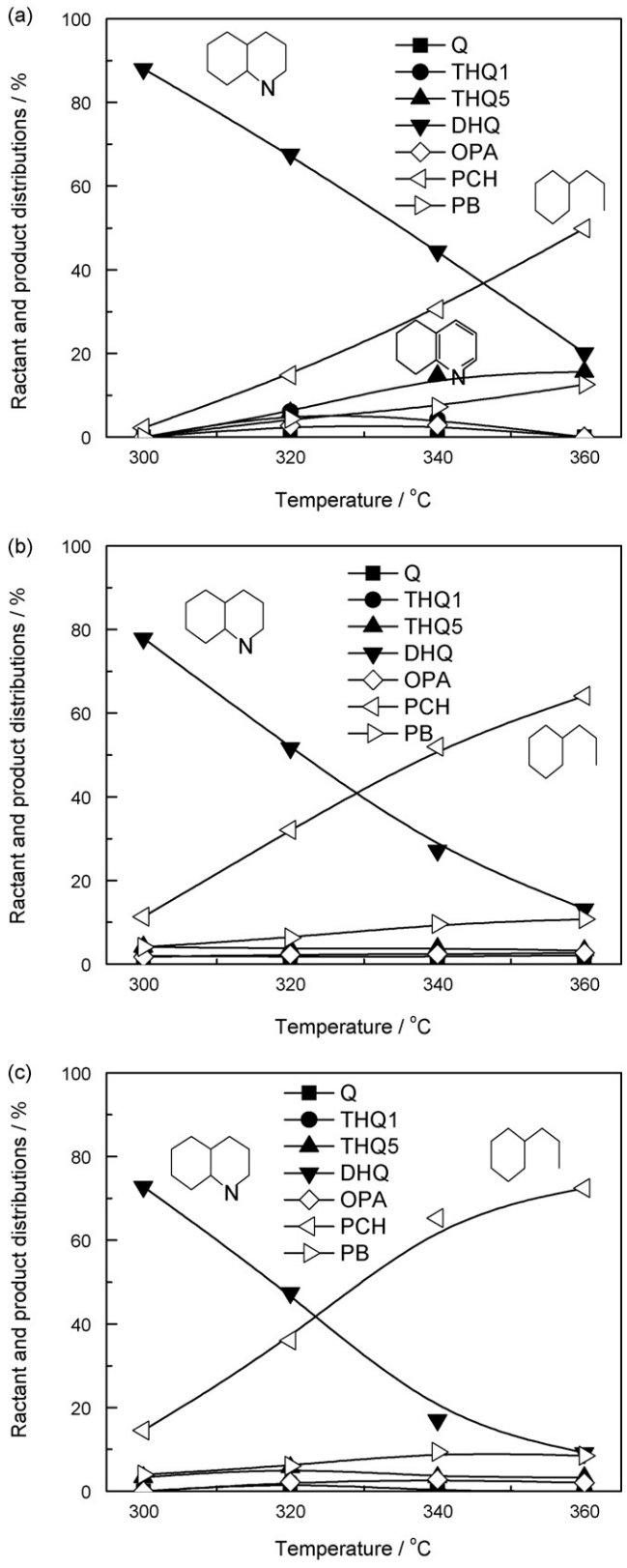


**Fig. 10.** Product distributions as a function of temperature in DHQ HDN over MoP/MCM-41 (a), MoP-Ti(5)/MCM-41 (b), and Ti(5)-MoP/MCM-41 (c).

Lewis acid sites of Ti(5)-MoP/MCM-41 can be attributed to the coverage of the MoP/MCM-41 surface acid sites by $TiO_2$ species.

XPS characterization revealed that the $TiO_2$ species on the surface of the Ti(5)-MoP/MCM-41 and MoP-Ti(5)/MCM-41 (Table 2) were much higher than the nominal atomic Ti/Mo ratios. It is suggested that Ti species may migrate to the surface of MoP in the preparation. The Ti $2p_{1/2}$ binding energy peak at 455.3 eV indicates the presence of partially reduced $Ti^{n+}$ ($n < 4$) species on both MoP-Ti(5)/MCM-41 and Ti(5)-MoP/MCM-41 [26]. The difference in the intensities of the two broad shoulder peaks indicated that more $Ti^{n+}$ ($n < 4$) species were presented in MoP-Ti(5)/MCM-41 than in Ti(5)-MoP/MCM-41.

In catalytic HDN, adsorption of nitrogen-containing molecules is a prerequisite. The adsorption configurations of the nitrogen-containing molecules may affect the HDN reactivity and the reaction pathways [29,30]. Quinoline can adsorb on a catalyst with the molecular plane parallel to the plane via a side-on adsorption, or with the molecular plane perpendicular via an end-on adsorption. This is consistent with our observations that THQ1 and THQ5 were the major partially hydrogenated intermediates of Q HDN and the dehydrogenation intermediates of DHQ HDN over MoP/MCM-41 (Figs. 8 and 10). The observed dehydrogenation activity of MoP/MCM-41 in DHQ HDN can be attributed to the metallic nature of the phosphide. Oyama [31] measured the MAS-NMR spectra of metal phosphides, and found that the NMR shift for the phosphides was a Knight shift resulting from the interaction of P nuclei with the conduction electrons of the solid. The shifts were different from the chemical shifts of phosphate, and showed the metallic nature of the phosphide. The concentration of THQ5 was much lower in DHQ HDN over MoP-Ti(5)/MCM-41 and Ti(5)-MoP/MCM-41, suggesting that the dehydrogenation activity of MoP/MCM-41 was suppressed by the addition of $TiO_2$.

Fig. 7 shows that the HDN TOF of MoP/MCM-41 in Q HDN was improved by the addition of $TiO_2$. The enhanced HDN TOF can be the result of the enhanced C–N cleavage activity or the hydrogenation activity of $TiO_2$-containing MoP/MCM-41. Because the C–N bond breaking occurs via DHQ, the concentration of hydrocarbons may increase when the reaction of THQ1 to DHQ is accelerated. Therefore, we investigated the HDN of DHQ to evaluate the denitrogenation performance of MoP/MCM-41, MoP-Ti(5)/MCM-41 and Ti(5)-MoP/MCM-41. Both MoP-Ti(5)/MCM-41 and Ti(5)-MoP/MCM-41 showed a much higher DHQ HDN TOF than MoP/MCM-41, indicating that the C–N bond cleavage activity of MoP/MCM-41 was improved by the addition of $TiO_2$. Although MoP-Ti(5)/MCM-41 exhibited higher Q HDN TOF than Ti(5)-MoP/MCM-41 (Fig. 7), their DHQ HDN TOFs were similar (Fig. 9). This suggests that MoP-Ti(5)/MCM-41 and Ti(5)-MoP/MCM-41 possess equally high C–N bond cleavage activity, whereas MoP-Ti(5)/MCM-41 has a higher hydrogenation activity.

Q and DHQ HDN results indicated $TiO_2$ is a promising promoter for MoP/MCM-41 in HDN. It is indicated that the C–N bond cleavage on MoP/MCM-41 was enhanced by the introduction of $TiO_2$. There are a few mechanisms dealing with C–N bond cleavage reactions, including nucleophilic substitution ($S_N1$, $S_N2$), elimination (E1, E2), and metallacycle or metal alkyl formation pathways [31]. The pathway involved in the reactions with metals requires the activation of the α-carbon to the nitrogen [32]. It is likely to occur on metallic catalysts such as Rh, Pd, and Ru, but not with phosphide or sulfide catalysts [27]. Hadjiloizou et al. [33] proposed two possible mechanisms for the opening of piperidine ring, i.e. E2 elimination and $S_N2$ substitution. Both acidic and basic sites are necessary in the elimination reactions [29]. Oyama and Lee [34] investigated the HDN of 2-methylpiperidine and 2,6-dimethylpiperidine over $Ni_2P/SiO_2$ and a commercial $NiMoS/Al_2O_3$. They suggested that the mechanism of HDN on phosphides was very similar to that on sulfides. Both substitution and elimination are evolved in the HDN over $Ni_2P/SiO_2$ whereas the predominant pathway in the HDN of 2-methylpiperidine is through substitution. However, for the more sterically hindered 2,6-dimethylpiperidine, the reaction proceeded mainly by E2 elimination. Abu and Smith

[16] studied the HDN of carbazole over $Ni_xMoP$ and MoP, and found that the selectivity to bicyclohexane was higher for $Ni_xMoP$ than for MoP. They attributed the enhanced C–N bond cleavage to the increase of the catalyst acidity. Nevertheless, the Py-IR results indicated that the acidity was not significantly affected by the introduction of $TiO_2$ in our study. It is assumed that the enhanced C–N bond cleavage activities of MoP-Ti(5)/MCM-41 and Ti(5)-MoP/MCM-41 may relate to the electronic interactions between Ti species and MoP phase. As evidenced by XPS measurement, $TiO_2$ in the MoP-Ti(5)/MCM-41 or Ti(5)-MoP/MCM-41 was partially reduced in the preparation. These low-valence Ti species may act as the electron donor, possibly transforming MoP phase to an electron-rich state. The increased electron density of MoP may be responsible for the enhanced HDN activities of MoP-Ti(5)/MCM-41 and Ti(5)-MoP/MCM-41. The electron-rich MoP species may enhance both the nucleophilic substitution and the abstraction of the β-hydrogen in the elimination reaction.

$TiO_2$ was considered as an electronic promoter in the conventional supported $MoS_2$ catalysts [18]. Under HDS reaction conditions, a fraction of the $Ti^{4+}$ species present in the support could be partially reduced to $Ti^{3+}$ species. The 3d electron in $Ti^{3+}$ is readily transferred through the conduction band, and injected into the Mo 3d conduction band, weakening the Mo–S bond and increasing the number of S vacancies. Our recent research [19] also showed the electronic interactions between the surface Ti species and $Ni_2P$.

## 5. Conclusion

$TiO_2$ is a promising promoter for MoP/MCM-41 in both Q and DHQ HDN. Addition of $TiO_2$ enhanced the C–N bond cleavage of MoP/MCM-41 whereas suppressed the dehydrogenation activity. The optimal $TiO_2$ loading was found to be 5 wt%. The TPR results indicated that introduction of $TiO_2$ enhanced the reduction of $Mo^{6+}$ to $Mo^{4+}$, but hardly influenced the formation of MoP phase. Both Ti(5)-MoP/MCM-41 and MoP-Ti(5)/MCM-41 possessed higher CO uptake than MoP/MCM-41. No significant differences in the acid properties and particle size distributions were observed between MoP/MCM-41 and the $TiO_2$-containing counterparts. XPS results revealed a surface enrichment of $TiO_2$ in Ti-containing catalysts, and a small amount of the surface $TiO_2$ was partially reduced to $Ti^{n+}$ ($n < 4$). It is suggested that these $Ti^{n+}$ ($n < 4$) species may be responsible for the promoting effect of $TiO_2$ on the HDN performance of MoP/MCM-41.

## Acknowledgements

The authors acknowledge the financial supports from the Natural Science Foundation of China (20333030, 20503003, and 20773020), NCET, and 111 Project. We thank Mr. Yongying Chen for assistance in characterization.

## References

[1] H. Topsøe, B.S. Clausen, F.E. Massoth, Hydrotreating Catalysis, Springer, New York, 1996.
[2] T. Kabe, A. Ishihara, W. Qian, Hydrodesulfurization and Hydrodenitrogenation, Chemistry and Engineering, Wiley-VCH, Weinheim, Germany, 1999.
[3] W.R.A.M. Robinson, J.N.M. van Gestel, T.I. Koranyi, S. Eijsbouts, A.M. van der Kraan, J.A.R. van Veen, V.H.J. de Beer, J. Catal. 161 (1996) 539.
[4] W. Li, B. Dhandapani, S.T. Oyama, Chem. Lett. (1998) 207.
[5] C. Stinner, R. Prins, T. Weber, J. Catal. 191 (2000) 438.
[6] A.E. Nelson, M. Sun, A.S.M. Junaid, J. Catal. 241 (2006) 180.
[7] S.J. Sawhill, D.C. Phillips, M.E. Bussell, J. Catal. 215 (2003) 208.
[8] V. Zuzaniuk, R. Prins, J. Catal. 219 (2003) 85.
[9] C. Stinner, R. Prins, T. Weber, J. Catal. 202 (2001) 187.
[10] P.A. Clark, S.T. Oyama, J. Catal. 218 (2003) 78.
[11] J.A. Rodriguez, J.-Y. Kim, J.C. Hanson, S.J. Sawhill, M.E. Bussell, J. Phys. Chem. B 107 (2003) 6276.
[12] A. Montesinos-Castellanos, T.A. Zepeda, B. Pawelec, E. Lima, J.L.G. Fierro, A. Olivas, J.A. de los Reyes H, Appl. Catal. A: Gen. 334 (2008) 330.
[13] D.C. Phillips, S.J. Sawhill, R. Self, M.E. Bussell, J. Catal. 207 (2002) 266.
[14] F. Sun, W. Wu, Z. Wu, J. Guo, Z. Wei, Y. Yang, Z. Jiang, F. Tian, C. Li, J. Catal. 228 (2004) 298.
[15] I.A. Abu, K.J. Smith, J. Catal. 241 (2006) 356.
[16] I.A. Abu, K.J. Smith, Catal. Today 125 (2007) 248.
[17] G. Murali Dhar, B.N. Srinivas, M.S. Rana, M. Kumar, S.K. Maity, Catal. Today 86 (2003) 45.
[18] J. Ramírez, L. Cedeño, B. Guido, J. Catal. 184 (1999) 59.
[19] X. Li, M. Lu, A. Wang, C. Song, Y. Hu, J. Phys. Chem. C 112 (2008) 16584.
[20] A. Wang, T. Kabe, Chem. Commun. (1999) 2067.
[21] A. Wang, L. Ruan, Y. Teng, X. Li, M. Lu, J. Ren, Y. Wang, Y. Hu, J. Catal. 229 (2005) 314.
[22] M. Jian, R. Prins, J. Catal. 179 (1998) 18.
[23] C.N. Satterfield, J.F. Cocchetto, Ind. Eng. Chem. Process Des. Dev. 20 (1981) 53.
[24] J. Ren, A. Wang, X. Li, Y. Chen, H. Liu, Y. Hu, Appl. Catal. A: Gen. 344 (2008) 175.
[25] S.-P. Sheu, G.K. Hellmut, R. Schlögl, J. Catal. 168 (1997) 278.
[26] Q. Fu, T. Wagner, S. Olliges, H.-D. Carstanjen, J. Phys. Chem. B 109 (2005) 944.
[27] S.T. Oyama, X. Wang, Y.-K. Lee, K. Bando, F.G. Requejo, J. Catal. 210 (2002) 207.
[28] Z. Wei, Q. Xin, X. Guo, E.L. Sham, P. Grange, B. Delmon, Appl. Catal. 63 (1990) 305.
[29] R. Prins, Adv. Catal. 46 (2001) 399.
[30] G. Perot, Catal. Today 10 (1991) 447.
[31] S.T. Oyama, J. Catal. 216 (2003) 343.
[32] K.J. Weller, P.A. Fox, S.D. Gray, D.E. Wigley, Polyhedron 16 (1997) 3139.
[33] G.C. Hadjiloizou, J.B. Butt, J.S. Dranoff, Ind. Eng. Chem. Res. 31 (1992) 2503.
[34] S.T. Oyama, Y.-K. Lee, J. Phys. Chem. B 109 (2005) 2109.